Volume 6 | Number 6 | June 2018 | Pages 1273–1656

Biomaterials Science

rsc.li/biomaterials-science

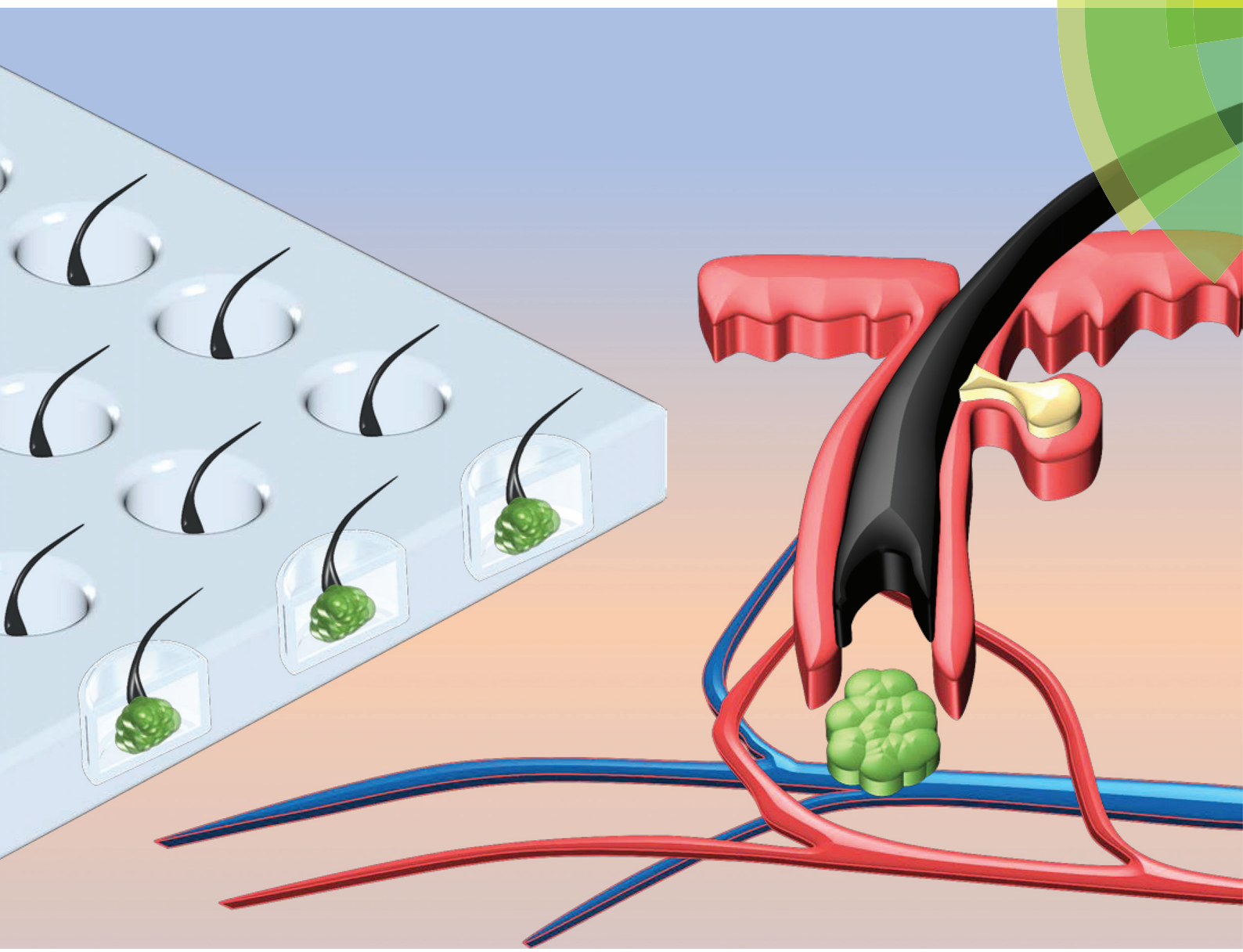

ISSN 2047-4849

ROYAL SOCIETY OF CHEMISTRY

PAPER
Lifeng Kang *et al.*
Impact of substrate stiffness on dermal papilla aggregates in microgels

European Society for Biomaterials

Biomaterials Science

PAPER

View Article Online
View Journal | View Issue

Cite this: *Biomater. Sci.*, 2018, **6**, 1347

Impact of substrate stiffness on dermal papilla aggregates in microgels

Justin J. Y. Tan,[a] Jie Kai Tee,[a,b] Keat Onn Chou,[a] Shi Ya Au Yong,[a] Jing Pan,[c] Han Kiat Ho,[a,b] Paul C. L. Ho[a] and Lifeng Kang *†[a]

Received 2nd March 2018,
Accepted 28th March 2018

DOI: 10.1039/c8bm00248g

rsc.li/biomaterials-science

Interaction between cells and the extracellular environment plays a vital role in cellular development. The mechanical property of a 3-dimensional (3D) culture can be modified to mimic *in vivo* conditions. Dermal papilla (DP) cells are shown to gradually lose their inductivity in hair cycle development in a 2-dimensional culture. They are shown to partially restore their inductivity when transferred into a 3D microenvironment. In this study, a microarray fabricated from three different concentrations of poly-ethylene-glycol-diacrylate 3500, namely 5%, 10% and 15% w/v, yielded increasing substrate stiffness. The impact of varying substrate stiffness was tested for DP cell viability, attachment, and selected hair inductive markers. DP aggregates were shown to be viable and exhibited greater spreading with increasing substrate stiffness. Moreover, DP aggregates cultured on a softer substrate showed a greater fold change of gene and protein expressions than those cultured on a harder substrate.

Introduction

Androgenetic alopecia (AGA) is characterized by a progressive and patterned transformation of thick, pigmented terminal scalp hairs into short, fine, hypo-pigmented vellus-like hairs.[1] Clinicians have long resorted to transplanting hair follicles to treat AGA.[2] However, possible damage to grafts may be attributed to factors including mechanical injury resulting from crushing by forceps, desiccation during extraction, dehydration, chemical solutions used for storage, heat and hypoxia.[3] These factors, combined with a dearth of donor hair follicles, greatly compromise the quality and the quantity of viable hair follicles available for transplantation.

To this end, current technologies have explored the possibility of regenerating hair follicles *in vitro* for transplantation.[2] The ability to induce hair follicle neogenesis in hairless skin is retained in cultured dermal papilla (DP) cells (a major component of hair follicles) but not their inductive ability, which tends to be lost during passaging.[4–6] When removed from their *in vivo* microenvironment to culture in a 2-dimensional (2D) environment, DP cells are shown to gradually lose their inductivity in hair cycle development.[7] However, they partially restore their inductivity when transferred from the 2D environment and cultured in a 3-dimensional (3D) matrix.[8–10]

To preserve the inductivity of DP cells, many researchers turned to 3D culturing to produce environments that imitate *in vivo* extracellular matrices. This is because the interaction between cells and the extracellular environment plays an important role in cellular morphology and development.[11] Current models have explored the use of several ultra-low attachment substrates to facilitate the self-assembly of DP cells into 3D organoid microtissues. Yen *et al.* exploited the differences in surface adhesiveness of DP cells and keratinocytes on poly(ethylene-*co*-vinyl alcohol) (EVAL) substrates to create heterotypic hybrid microtissues with a central DP core and keratinocytes preferentially sorted to the periphery, resulting in the upregulation of keratin 6 and other markers suggesting epidermal differentiation towards a follicular fate.[12] Hsieh *et al.* have demonstrated the use of another low attachment material, namely, a polydimethylsiloxane (PDMS) microarray to produce large quantities of 3D DP microtissues expressing DP markers such as α-smooth muscle actin (α-SMA) and neural cell adhesion molecule (NCAM).[13] Huang *et al.* used hydrophilic polyvinyl alcohol (PVA), which is poorly adhesive to DP cells, thereby encouraging greater compaction of cells to produce denser aggregates with relatively good cell viability and expressing important DP markers such as versican and alkaline phosphatase.[10] However, the effects of substrate stiffness on DP expression of hair inductive gene and protein markers are not well-elucidated.

In this article, we show that DP cells respond to one of the key parameters of *in vivo* microenvironmental stimuli, namely

[a]*Department of Pharmacy, National University of Singapore (NUS), Lower Kent Ridge Road, 18 Science Drive 4, Singapore 117543, Singapore*
[b]*NUS Graduate School for Integrative Sciences and Engineering (NGS), Centre for Life Sciences (CeLS), #05-01, 28 Medical Drive, Singapore 117456*
[c]*Skinetrate Pte. Ltd., Singapore, A*StartCentral, Blk 79 Ayer Rajah Crescent #05-03, Singapore 139955, Singapore*
†Current affiliation: Faculty of Pharmacy, University of Sydney, Pharmacy and Bank Building A15, NSW 2006, Australia. E-mail: lifeng.kang@sydney.edu.au

mechanical stiffness. In our group, we used poly-ethylene-glycol-diacrylate (PEGDA) to fabricate microgels to mimic the hair follicular microenvironment.[14,15] The mechanical stiffness of the microgels can be varied by changing the PEGDA concentration to produce a range of microgels with increasing stiffness.[16] In native tissues, DP cells are located at the base of hair follicles.[17] It was reported that the mechanical stiffness of hair follicles was found to be softer at the base than at the upper segments, with an elastic modulus of approximately 30 kPa.[18] Therefore, we hypothesize that soft hydrogels can better preserve the inductivity of DP cells than hard hydrogels.

In this study, microgels are prepared by using PEGDA with varying stiffness and their effects on the DP cell viability, morphology, and gene/protein expressions are investigated (Fig. 1).

Experimental

Polydimethylsiloxane (PDMS) stamp fabrication

Prepolymer siloxane elastomer base solution was mixed with the curing agent Sylgard 184 (Dow Corning Corporation, Midland, USA) at a 10 : 1 ratio by mass. The PDMS prepolymer mixture was poured onto a silicon master with an SU-8 photoresist coating patterned with an array of 200 μm (diameter) microwells and degassed for 20–25 min in a vacuum chamber to remove any air bubbles before curing at 70 °C for 2 h. The PDMS layer was peeled off from the silicon master and cut to a suitable size. The resulting PDMS stamp had patterns corresponding to the silicon master in the form of micropillars with diameters of 200 μm each, and was imaged using a stereomicroscope (Nikon SMZ25, Japan).

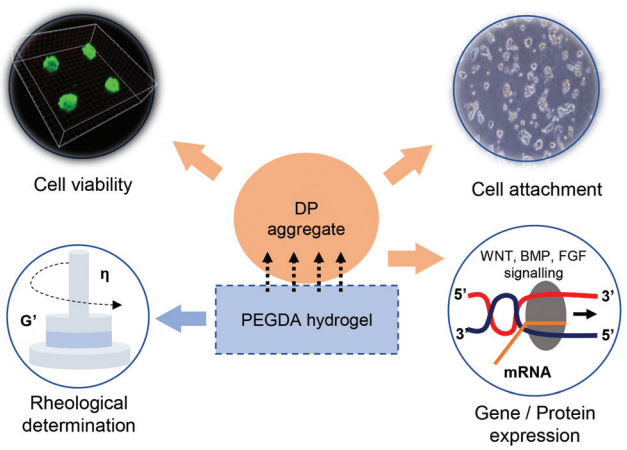

Fig. 1 Schematic representation of the workflow. The PEGDA composition was varied to yield gels of varying stiffness. Microwells were microfabricated to enable DP cells to form microspheres. Their cell viability and substrate adhesion behavior were observed, and subsequently their expression of key inductive genes was quantified and compared.

PEGDA microwell array fabrication

UV-photocrosslinkable PEGDA (Jenkem Technology, USA) with a molecular weight (MW) of 3500 Da was mixed with the photoinitiator Irgacure 2959, 2-hydroxy-4′-(2-hydroxy-ethoxy)-2-methylpropiophenone (HHEMP) (Sigma-Aldrich, USA) and diluted with 1× PBS to form a prepolymer solution comprising the photoinitiator of the respective % w/v as reported in Table 1. The ratio of PEGDA : HHEMP for each substrate was kept constant at 20.

The patterned PDMS stamp was placed on an evenly distributed film of prepolymer solution on a 3-trimethoxysilyl propyl methacrylate (TMS-PMA) (Sigma-Aldrich, USA)-treated cover slip, with 2 coverslips placed on both sides as spacers. Photopolymerization was achieved by irradiating the set-up with UV light of 320–500 nm and at an intensity of 4.96 W cm^{-2} for 30 s using the OmniCure®Series 2000 curing station (Lumen Dynamics, Canada) as previously optimized. After photopolymerization, the PDMS stamp was peeled from the fabricated hydrogel microwell arrays, which were submerged in 70% ethanol for 2 h to remove excess prepolymer solution. Hydrogel microwell arrays were subsequently washed thrice and stored in sterile PBS under aseptic conditions prior to cell seeding. The microwell arrays were then assessed for their suitability to be used in the seeding of the DP cells.

Rheology determination of PEGDA hydrogels

The flat surface of the PDMS stamp was placed on an evenly distributed film of prepolymer solution on an untreated glass slide, with 2 coverslips placed on both sides as spacers. Photopolymerization was performed using the same conditions mentioned earlier. The rheological property of the PEGDA hydrogel samples was measured using a modular rheometer MCR302 (Anton Paar, Austria) with an 8 mm diameter parallel-plate (PP08). The PEGDA sample was loaded onto the stand and trimmed to fit the shape of the parallel-plate, before commencing on an amplitude sweep test. The amplitude sweep test was conducted at a constant angular frequency of 10 rad s^{-1} with a logarithmic shear strain ramp from 0.01% to 100%. The upper plate was lowered very slowly while monitoring the normal force and was stopped at a limit normal force of 0.25 N. The test temperature was maintained at 37 °C by using a Peltier temperature device. Three replicates of each PEGDA composition are

Table 1 Fabricated PEGDA 3500 microwell arrays and their corresponding components

Substrate	Composition of PEGDA (%w/v)	Weight of PEGDA (mg)	Volume of HHEMP (μL)	Final volume (μL)	Final conc. of HHEMP (%w/v)	Ratio of PEGDA : HHEMP
S1	5	50	950	1000	0.09	20
S2	10	100	900	1000	0.18	20
S3	15	150	850	1000	0.27	20

used for the rheological measurement. The information obtained from the flow diagram of the PEGDA substrates was then used to approximate the elastic moduli of the substrates to compare with the elastic moduli of the hair follicles.[18–20]

$$G^* = G' + iG'' \quad (1)$$

Storage modulus G' and loss modulus G'' are related to complex shear modulus G^* in eqn (1). The storage modulus is a measure of stored energy in the material, and the loss modulus is a measure of energy loss during the test. The first term usually relates to elasticity while the second relates to viscosity. G^* is therefore a term with a real and an imaginary component.

$$\text{Loss tangent} = \tan\delta = \frac{G''}{G'} \quad (2)$$

To calculate the complex shear modulus, the loss tangent is first calculated using eqn (2). Phase angle δ, which is the phase lag between the shear stress and the strain measured during the testing, is then calculated from the loss tangent.

$$G' = G^* \cos\delta \quad (3)$$

$$G'' = G^* \sin\delta \quad (4)$$

The complex shear modulus is related to the storage modulus and the loss modulus in eqn (3) and (4). It can be calculated by substituting phase angle δ into either eqn (3) or (4). Both equations will give the same value of the complex shear modulus.

$$G^* \approx G' \approx G \text{ if } \tan\delta < 0.2$$

If the loss tangent is less than 0.2, then the loss modulus will be very small, and the complex shear modulus will be approximately equal to the storage modulus. This G^* value can be a good approximate for shear modulus G.[20,21]

$$E = 2G(1+\nu) \quad (5)$$

Elastic modulus (E) is related to shear modulus in eqn (5), where ν is Poisson's ratio. Poisson's ratio is the ratio of the lateral and the longitudinal strains when the material is sheared. Poisson's ratio of most hydrogels is assumed to be around 0.45–0.5, meaning the $E \approx 3G$.

Cell culture

The immortalized dermal papilla cell line was donated by Professor Mike Philpott and Dr Adiam Bahta from Queen Mary University London for this work. The cell lines were previously isolated and immortalized from dermal papilla cells obtained from scalp biopsy.[22] The immortalized human dermal papilla cell line (p33) was manipulated under aseptic conditions and maintained in a humidified incubator at 37 °C and 10% CO_2. Culture media consisted of Dulbecco's modified Eagle's medium (DMEM) (Invitrogen Corporation, USA) supplemented with 10% fetal bovine serum (FBS) (Invitrogen Corporation, USA) and 1% penicillin–streptomycin (10 000 U mL^{-1} penicillin and 10 mg mL^{-1} streptomycin, PAN-Biotech GmbH, Germany). All media components were sterilized *via* filtration through 0.22 μm pore Corning filter units (Corning Incorporated, USA). Culture medium was changed every 3 days and cells were passaged when flasks were 80–90% confluent.

Cell seeding and aggregate formation

Expanded DP cells were seeded into the microgels using the wiping method as previously reported.[23] Briefly, 15 μL DP cell suspension (12 million cells per mL) were pipetted along the edge of a cover slip, which was then slowly wiped across each array. Microwell arrays seeded with DP cells were left to stand for 5 min for the cells to settle into the microwells, before being cultured with culture medium in a humidified incubator at 37 °C and 5% CO_2. Aggregate formation inside the microwells was observed and imaged using an inverted microscope (Leica DM IL, Germany). 2D DP cultures were also carried out in Petri dishes (Thermo Scientific, USA) to serve as a comparison against 3D DP cultures. To mimic the same number of cells in the microwell arrays for the 2D DP culture, an estimate was obtained from the equation published in an earlier work.[23]

Cell viability using a live/dead assay

The cell viability of seeded microwell arrays was assessed using a live/dead staining kit (Invitrogen Corporation, USA) on day 2. DP cells were incubated in 4 μM ethidium homodimer (EthD) and 2 μM calcein acetoxymethyl ester (calcein-AM), diluted in phosphate buffered saline (PBS), for 10 min at 37 °C and subsequently imaged using a fluorescence microscope (Nikon Eclipse Ti-U, Japan, ex: 545–565 nm). Live cells appear green due to enzymatic conversion of calcein-AM to fluorescent calcein while dead cells appear red after binding of EthD to nucleic acids in cells with damaged plasma membranes. To quantify cell viability, fluorescence intensities for both green and red colors were measured using Imaris software. Cell viability was calculated as the percentage ratio between green fluorescence reading and the sum of green and red fluorescence readings.

Cell attachment assay

Different wells from a 24 well plate (Greiner bio-one, Austria) were coated with 300 μL PEGDA at concentrations of 5% (S1), 10% (S2) and 15% (S3) and cured under UV light of 320–500 nm and at an intensity of 4.96 W cm^{-2} for 30 s using the OmniCure®Series 2000 curing station. Wells that were not coated with PEGDA were used as a reference control for 2D cell culture. These are normal, non-treated wells in the 24 well plate. DP cells were seeded at 50 000 cells into the respective wells and incubated for 6 h and 24 h, respectively. Non-adherent cells were washed away with PBS 6 h and 24 h after cell seeding. Attached cells were detached by trypsin/EDTA and counted by using a hemocytometer in 500 μl per sample.

mRNA extraction

mRNA was extracted from cells using an RNeasy mini kit in accordance with the manufacturer's instructions. The concentration of mRNA was determined using a Nanodrop 1000 Spectrophotometer (Thermo Scientific, USA). Reverse transcrip-

tion of total mRNA was performed at 1 μg total mRNA in 20 μL final volume using random primers and avian myeloblastosis virus reverse transcriptase. The concentrations of complementary deoxyribonucleic acid (cDNA) after reverse transcription were also determined using a Nanodrop spectrophotometer.

Quantitative real-time polymerase chain reaction (PCR)

Quantitative real-time PCR reaction was performed using a Rotor-Gene Q real time PCR cycler (Qiagen, Germany). Primers from Integrated DNA Technologies, Singapore were used for PCR reactions. The primer sequences were designed using Primer3 (http://frodo.wi.mit.edu/) and Primer-BLAST (http://www.ncbi.nlm.nih.gov/tools/primer-blast/).

A beta actin primer was also included as an internal loading control. Each reaction mixture was prepared using 10 μL QuantiFast SYBR Green PCR master mix, 4 μL cDNA template and 1 μM of each primer in a total reaction volume of 20 μL. The PCR was run for 40 cycles and the thermal cycling conditions were as follows: initial heat activation at 95 °C for 10 minutes; denaturation for 10 seconds at 95 °C; and combined primer annealing and extension for 60 seconds at 60 °C. The fluorescence signal was measured at the end of each extension step. After the amplification, a melting peak analysis with a temperature gradient from 72 °C to 95 °C was performed. Fluorescence emission readings were analyzed using Rotor-Gene Q software (Qiagen, Germany). The data were presented as the fold increase of the target gene expression, normalized to the housekeeping gene beta-actin.

Western blotting

Radioimmunoprecipitation assay (RIPA) buffer containing 0.1% sodium dodecyl sulfate (SDS), 0.5% sodium deoxycholate and 1% NP-40 was added to the cells and incubated on ice for 15 min. Cell lysates were then loaded into 10% acrylamide gel (Bio-Rad) and run at 130 V for 2 hours. The proteins were transferred onto a PVDF membrane (Thermo Scientifc) at 100 V for another 2 hours. Subsequently, the blots were blocked with 5% bovine serum albumin (BSA) in Tris-buffered saline containing 1% Tween-20 (TBST, 1st Base) for 1 hour before overnight incubation at 4 °C with Axin-2 (2C10), BMP-4 (3H2.3), Noggin (2C10) and β-actin (C4) mouse primary antibodies (Santa Cruz). After washing three times with TBST, the blots were further incubated with anti-mouse antibodies (Cell Signaling) for 1 hour at room temperature. The blots were further washed with TBST additional three times and developed with a Western Lightning Plus-ECL reagent (PerkinElmer) using a G:Box Gel imaging system (Syngene). Quantification of band intensities was done using Image J software and normalized to housekeeping β-actin expression, and subsequently, comparisons were made by normalizing individual values to 2D culture expression values. Experiments were performed for at least three replicates.

Statistical analysis

Results were expressed as means ± standard deviation of at least three independent experiments. Statistical analysis was performed by one-way analysis of variance (ANOVA). The difference was statistically significant at a p-value of <0.05.

Results

Fabrication of a PEGDA hydrogel microarray

The polydimethylsiloxane (PDMS) stamp was fabricated using a silicon master with an SU-8 photoresist coating patterned with microwells according to the steps outlined in Fig. 2A. The PEGDA hydrogel microwell arrays were then fabricated on the top of 3-trimethoxysilyl propyl methacrylate (TMS-PMA) treated coverslips, using the PDMS stamp as a mold, as shown in Fig. 2B, *via* ultraviolet (UV) initiated crosslinking of diacrylate groups, from prepolymer solution containing 5%, 10% or 15% w/v PEGDA MW 3500 and the corresponding amounts of the 2-hydroxy-4′-(2-hydroxy-ethoxy)-2-methylpropiophenone (HHEMP) photoinitiator. Using the PDMS stamp as a mold, microwells with a diameter of 200 μm each were formed as shown in Fig. 2C (cross-sectional view of the PEGDA microarray). In general, our methods allowed consistent and rapid fabrication of PEGDA hydrogel microwell arrays: firstly, a single PDMS stamp was used to fabricate all the hydrogel microwell arrays, thus ensuring consistency in the size and shape of the molded microwells and secondly, fabrication *via* UV photo-polymerization takes only 30 s for each microwell array. Each hydrogel microarray contained 15 by 15 microwells, hence allowing the seeding and subsequent formation of 225 DP aggregates.

Rheological determination of PEGDA hydrogels

The storage modulus of a higher concentration of the PEGDA material in the hydrogel was found to be higher than that of a lower concentration. There was statistical significance between the storage moduli of the hydrogels of different concentrations. The 5% hydrogels showed the longest linear viscoelastic region than the other hydrogels, thus having the highest yield point, which is the maximum limit of a linear viscoelastic region of a material, amongst the substrates. The flow point of 10% hydrogels, which is the intersection of the storage modulus G' and loss modulus G'' curves, was also found to be at a higher percentage of shear strain and a lower G' value than the flow point of 15% hydrogels. In contrast, the storage modulus G' and loss modulus G'' curves of 5% hydrogels did not intersect within the range of shear strain applied. The estimated elastic moduli followed the same trend as the storage moduli and statistical significance were also found among the PEGDA hydrogels (Fig. 3).

Characterization of the microwells

The diameters of the microwells for substrates made from varying compositions of PEGDA, namely S1 (5%), S2 (10%) and S3 (15%), were measured on day 0 and day 2 after seeding of the DP cells. The diameters of the microwells remained non-significantly different across S1–S3 over the course of 2 days ($p > 0.05$). The measurements can be found in Table 2.

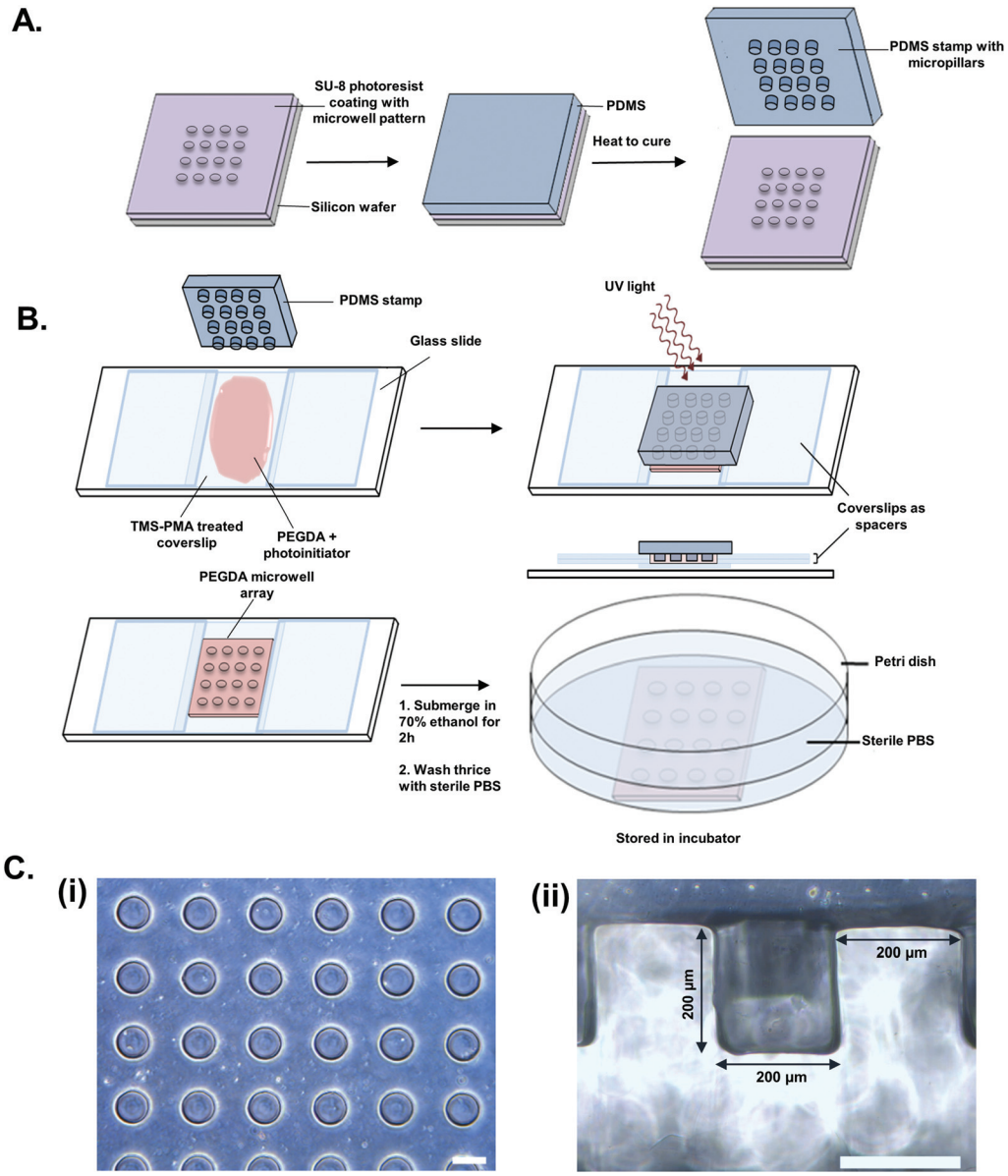

Fig. 2 Fabrication of PDMS stamps and PEGDA hydrogel microwell arrays. (A) A schematic diagram to illustrate fabrication of PDMS stamps using silicone elastomer base solution with the curing agent Sylgard 184 on a silicon master patterned with microwells. (B) A schematic diagram to illustrate fabrication of hydrogel microwell arrays by placing PDMS stamps on PEGDA with the photoinitiator HHEMP on the top of TMS-PMA treated coverslips. (C) (i) A top view of the PEGDA hydrogel microwell array at 5× magnification showing uniform wells with diameters of 200 µm each. (ii) A cross section of a single PEGDA 3500 hydrogel microwell. The dimensions of the microwell are as follows: depth = spacing between microwells = diameter = 200 µm. All scale bars represent 200 µm.

Cell viability

The cell viability of DP aggregates in the PEGDA hydrogel microarray was determined using a live/dead staining assay. Fig. 4A shows live/dead assay images of DP cell aggregates as 3D cultures in S1, S2 and S3, respectively. Cell viability was quantified by measuring the percentage ratio of fluorescence intensity from live cells over total fluorescence intensity from live and dead cells. Overall cell viability remained high for day 2 and no statistically significant difference in cell viability was observed between 3D cell aggregates across the different PEGDA substrates over 48 h ($p > 0.05$). This showed that the PEGDA hydrogel microwells were biocompatible, making this a suitable method for 3D culture of DP cells.

Cell attachment and spreading

DP cells generally exhibit lower attachment and spreading to PEGDA hydrogels of lower stiffness. Fig. 4B(i) and (ii) show that cells on 2D uncoated wells exhibited the greatest substrate adherence and spreading as compared to S1–S3. Fig. 4C shows the increasing extent of attachment and spreading behavior of

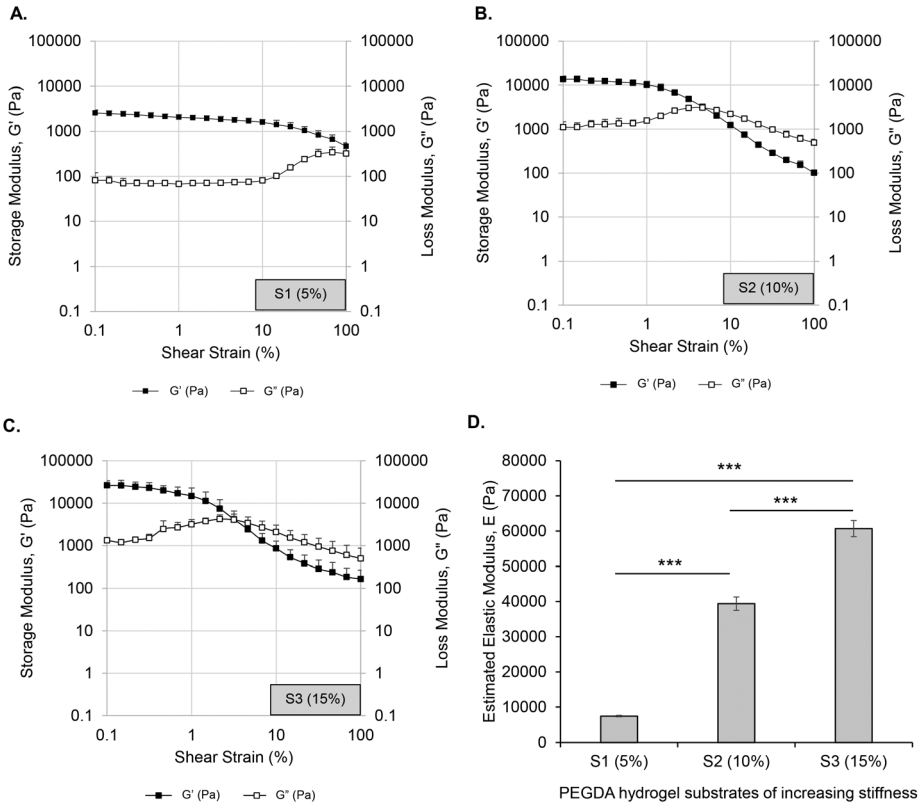

Fig. 3 Rheology results of PEGDA hydrogel samples. (A)–(C) A flow diagram of PEGDA 3500 5% (S1), PEGDA 3500 10% (S2) and PEGDA 3500 15% (S3), respectively. (■) represents the storage modulus (G') while (□) represents the loss modulus (G''). (D) Comparison of estimated elastic modulus (E) across various PEGDA compositions calculated with G' and G'' values within the linear viscoelastic region (LVE). All testing is carried out at a physiological temperature of 37 °C (n = 3). Statistical significance is determined using the ANOVA test. $p < 0.001$ is denoted with ***.

Table 2 Diameters of the hydrogel microwells (n = 18, 6 wells from each sample, total 3 samples for each PEGDA 3500 substratum)

		Average diameters of hydrogel microwells (μm) ± SD	
		Day 0	Day 2
PEGDA 3500 hydrogel of increasing stiffness	S1	188.37 (±5.59)	187.36 (±3.84)
	S2	190.16 (±2.14)	191.52 (±4.39)
	S3	188.59 (±2.54)	188.80 (±3.06)

DP cells when cultured on flat hydrogels as well as in 3D microwells. Fig. 4B(ii) shows the number of DP cells remaining on the respective substrates 6 h and 24 h post-incubation after washing. The number of adhered cells after washing with phosphate buffered saline (PBS) on uncoated PEGDA wells was significantly more than the numbers of cells seeded on the top of the PEGDA substrates of varying concentrations ($p < 0.05$). The number of cells seeded on S3 showed a greater number of adhered cells after washing as compared with cells seeded on S1 and S2 at 24 h but not at 6 h, suggesting that the DP cells take a longer time to adhere to the substrate, hence a higher number of cells remaining in the wells post-washing at 24 h as compared to 6 h for the hydrogel substrates. However, S1–S3 still showed much fewer number of adhered cells as compared to those cultured on 2D uncoated wells because of the hydrogels' inherent "low-attachment" characteristic towards cells as compared to the normal, untreated wells in the 24-well plate. An observation under a light microscope shows that DP cells exhibited increasing degrees of cell spreading when seeded on the top of PEGDA substrates of increasing stiffness.

Quantitative real-time polymerase chain reaction (PCR)

The qPCR results were obtained and compared using ΔΔCT analysis to obtain the fold change difference of each individual genes between DP cells grown in 3D hydrogels and 2D cultures. Fig. 5 shows that qPCR results had higher fold changes for the expression of most of the genes in the 3D model than in the 2D culture. DP cells grown in PEGDA 3500 15% gels (S3) exhibited expression of the genes similar to that in the 2D culture. Statistical significance fold changes for most of the gene markers of DP cells grown on PEGDA 3500 5% and 10% substrates were much higher than those of 15%. Statistical significance was not found between fold changes of the 10% (S2) and 5% substrates (S1), except in the case of BMP6 and Noggin.

Western blotting

Western blotting was employed to determine the protein expression of selected key markers for DP inductivity – *i.e.*, Axin2,

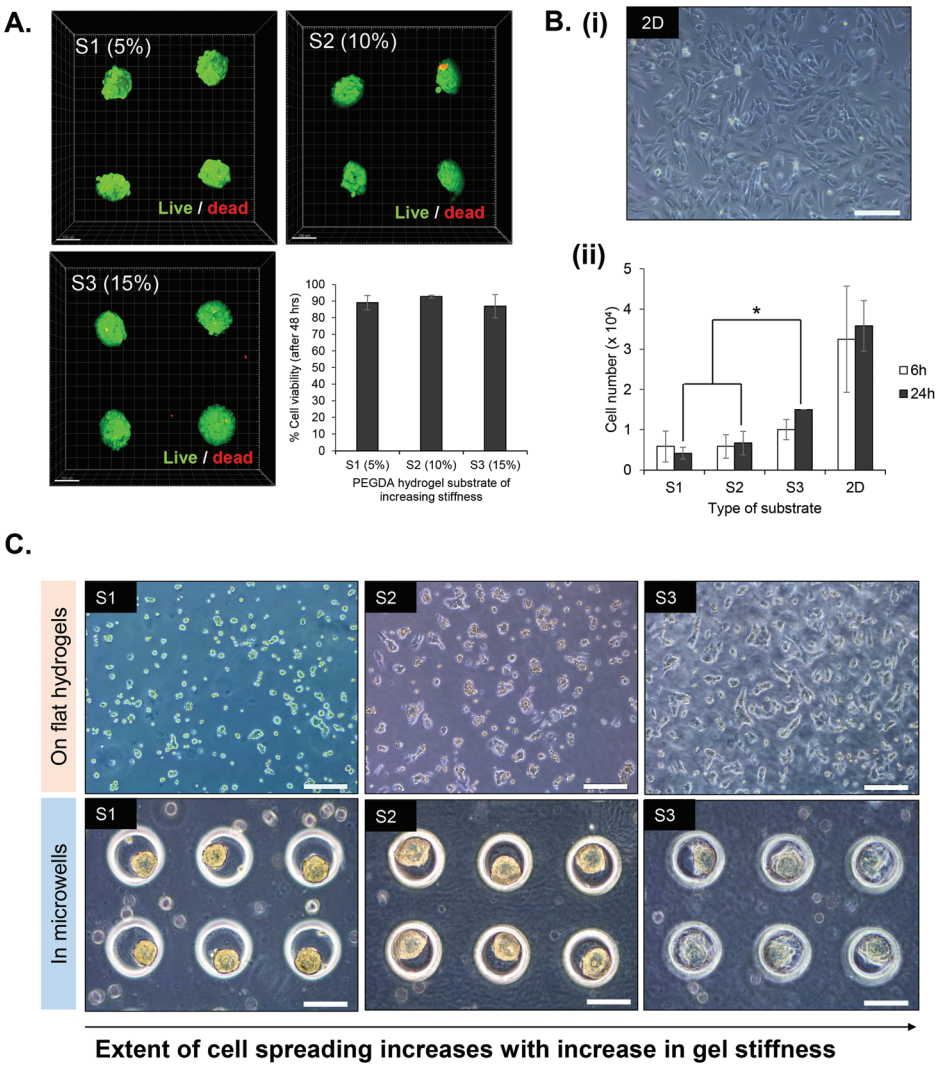

Fig. 4 (A) Live/dead staining for aggregates on PEGDA gels of varying stiffness. Cell viability in each aggregate is determined as a percentage of green intensity (calcein AM) over the sum of green and red (ethidium bromide) intensities, indicating live and dead cells, respectively (n = 12). (B) (i) An image of DP cells on a 2D uncoated well without a hydrogel substrate; (ii) number of DP cells remaining on PEGDA hydrogels of increasing stiffness from S1 to S3 as compared to 2D uncoated wells at 6 h and 24 h incubation, respectively. Statistical significance is determined using the one-way ANOVA test followed by *post-hoc* Turkey HSD. $p < 0.05$ is denoted with *. (C) The morphology of the DP seeded on flat hydrogels of increasing stiffness at 24 h and the morphology of DP aggregates in PEGDA hydrogels of increasing stiffness at 48 h. Scale bar = 200 μm.

BMP4 and Noggin. DP aggregates cultured on substrates S1, S2 and S3 – of increasing stiffness – were each normalized to the expression of their corresponding housekeeping β-actin protein. Comparisons in these protein expressions were made between 3D DP aggregates cultured on substrates of varying stiffness as well as against DP cultured on flat 2D cultures. Fig. 6 shows that the expression of Axin2, BMP4 and Noggin all favours 3D DP aggregates cultured on a softer substrate (S1) as compared to stiffer substrates (S2 and S3) and 2D cultures. The overall trend of protein expression was observed to be highest in S1, followed by S2 and S3, with S3 showing levels of protein expression similar to those yielded from 2D cultures. Axin2 and Noggin expressions were significantly higher in S1 as compared to the rest of the other substrates and 2D culture, while BMP4 expression was significantly higher in S1 as compared to S3 and the 2D culture.

Discussion

To consider whether the hydrogels were suitable for the seeding of DP cells for further experimentation, the hydrogel arrays were assessed visually, and their diameters measured using a stereomicroscope (Nikon SMZ25, Japan) at day 0 and day 2 as given in Table 2. The diameters of the microwells prepared from varying percentages of PEGDA – S1 (5%), S2 (10%) and S3 (15%) – showed non-significance ($p > 0.05$). As such, these PEGDA 3500 hydrogels were deemed suitable to be used in subsequent experimentation.

The viscoelastic properties of PEGDA 3500 hydrogels were analyzed. A higher concentration of the PEGDA material in the hydrogel component resulted in a higher G' modulus. With more PEGDA in prepolymer solution, the polymerization

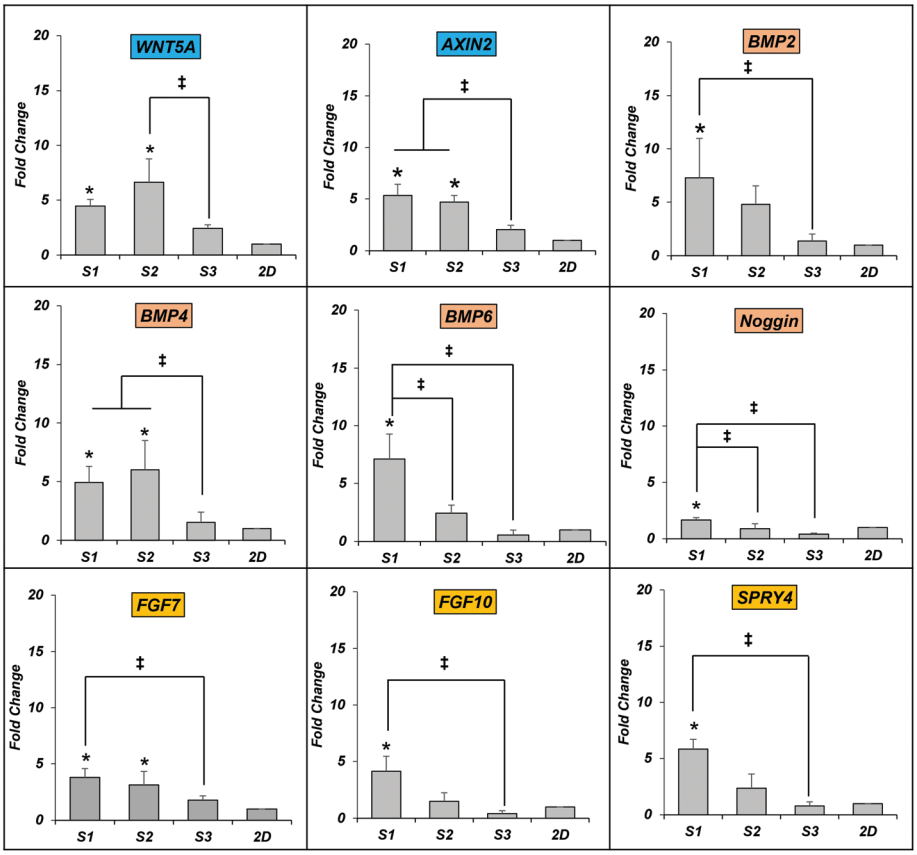

Fig. 5 The fold change of gene expression of 3D DP aggregates cultured on PEGDA hydrogels of increasing stiffness (S1 being the least stiff and S3 being the stiffest) normalized to the DP in the 2D culture (n = 3). The fold change is determined by comparing the individual gene expression, corrected with beta-actin expression, for both the 2D and 3D culture. Statistical significance is determined using the one-way ANOVA test followed by *post-hoc* Turkey HSD. $p < 0.05$ is denoted with * or ‡ as compared with the 2D culture or between 3D cultures, respectively.

between PEGDA became more extensive.[16] This resulted in a hydrogel substrate that was stiffer than the one made with a lower percentage of PEGDA. Statistical significance was found between the storage moduli of the three compositions of PEGDA 3500. This accentuated the fact that different percentages of PEGDA would result in substrates of different physical properties. PEGDA 3500 15% hydrogels (S3) were displayed to have shorter linear viscoelastic regions than PEGDA 3500 5% (S1) or 10% hydrogels (S2); this meant that the former had lower yield points than the latter. A higher yield point conferred strength to the hydrogels, allowing the hydrogels to withstand deformation at higher shear stress and exhibiting more elastic characteristics.[24]

The intricate relationship between the mechano-physical properties of the hydrogels and the effects of these properties on DP cells was the main objective of this paper. It was explored that the PEGDA hydrogels were generally non-toxic to the DP aggregates, and increasing the stiffness of the PEGDA hydrogels showed non-significant results to their cell viability.

The molecules from three well-established pathways of hair follicle induction, namely, the WNT pathway, the BMP pathway and the FGF pathway, were selected for this investigation.[25] These molecules were known markers present within the human DP cells.[25–27] They included ligands such as Wnt5A, BMP2, BMP4, BMP6, FGF7 and FGF10, downstream transcription factors such as AXIN2, and inhibitors such as Noggin and SPRY4. The upregulation of these molecules was seen essential for hair morphogenesis/regeneration as previously reported and their upregulation may imply that these pathways were active and held in check by their respective inhibitors.[28–31]

The WNT pathway was reported that its termination within the DP drastically reduced proliferation of the progenitors responsible for the regeneration of the hair shaft, leading to its premature destruction phase in hair follicle cycling.[28] BMP signaling was known to control the initiation of the growth phase in the hair follicle cycle and also in the regulation of apoptosis-driven hair follicle involution in postnatal hair follicles.[32] Many studies have proved the crucial role of FGF signaling in hair follicle development, such as FGF10 knockout mice that failed to grow whiskers and no hair growth phenotype in mice ablated of a functional FGF7 gene.[33,34] The interplay of these expressed hair inductive markers plays a huge role in initiating the new hair cycle in DP cells.

Gene expression analysis has demonstrated that the WNT/β-catenin activity in the DP regulates other signaling pathways

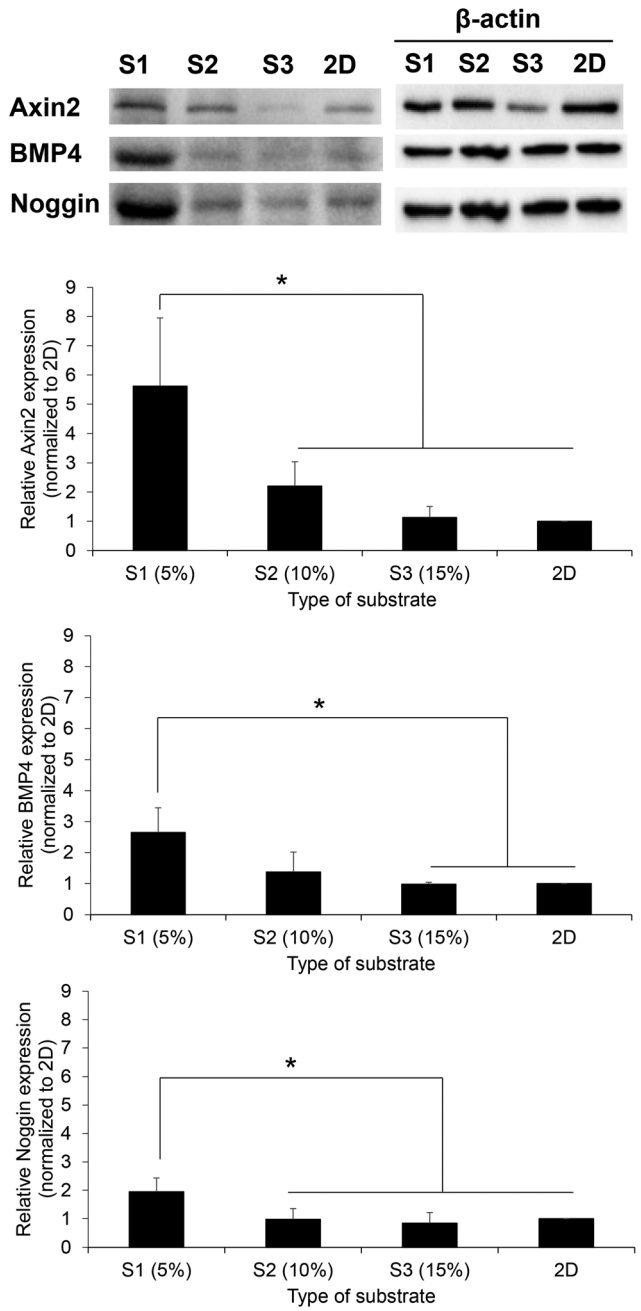

Fig. 6 Western blot analysis of Axin2, BMP4, Noggin and β-actin proteins from DP aggregates cultured on substrates of increasing stiffness, *i.e.* S1, S2 and S3, and 2D cultures. Total cell lysates were extracted using RIPA buffer containing 0.1% sodium dodecyl sulfate (SDS), 0.5% sodium deoxycholate and 1% NP-40. Quantification of the blots is summarized into graphs. Images were scanned using a G:Box Gel imaging system (Syngene) and quantified using Image J software. The data are expressed as a ratio of each protein to the housekeeping β-actin protein, normalized to the 2D culture (mean ± SD). Statistical significance is determined using the one-way ANOVA test followed by *post-hoc* Turkey HSD. $p < 0.05$ is denoted with *.

as well, including the FGF and the BMP signaling pathways.[28] The interplay between genes of these pathways may suggest that the upregulation of the markers of the WNT signaling – primarily WNT5A and AXIN2 in the DP cultured in softer substrates – *i.e.*, S1 and S2, might have influenced similar upregulation trends in the BMP and FGF signaling as well, giving rise to their upregulation. In contrast, a weaker expression of markers for the WNT signaling pathway in the DP aggregates cultured on a stiffer substrate, *i.e.*, S3, may have led to a weaker overall expression in the markers for BMP and FGF signaling. As indicated in Fig. 5, a higher composition of PEGDA in the hydrogels seemed to correlate with a weaker gene expression by the DP cells. The results of gene expression were confirmed with western blotting as shown in Fig. 6, whereby the expression of Axin2, BMP4 and Noggin were more abundant when the DP aggregates were cultured on a softer substrate as compared to harder substrates. As demonstrated in Fig. 4C, softer substrates encouraged DP aggregation while harder substrates resulted in greater attachment and spreading among the DP cells and aggregates. Previous studies have shown to correlate increasing cell spreading with increasing substrate stiffness.[35,36] Cells are known to spread more on stiffer gels as proven in many hydrogels like polyacrylamide (PAA) gels and polyethylene glycol (PEG) gels.[37,38] On the other hand, the phenomenon of tissue compaction is a known quality of cells grown on substrates promoting intercellular aggregation.[10] Substrates that promote greater intercellular aggregation tend to produce aggregates which are rounder, more spherical and more compact in nature. The diameters/sizes of these aggregates are reported to be reduced as a result of tissue compaction.[39] The increase in cellular aggregation may explain the higher upregulation of the gene expression within DP aggregates cultured on S1 rather than on S3. However, it is not clear if better DP aggregation is the primary reason for the upregulation of essential pathways responsible for DP inductivity or the DP aggregates generally responded better to softer substrates.

Stiffness of the ECM was shown to affect the differentiation of mesenchymal stem cells.[37] Softer substrates were found to be more supportive for adipogenic differentiation.[40] Similarly, the softer hydrogel might provide a better mimic of the DP-cell native environment as the elastic modulus nearer to the bulb of the hair was found to be much lower than upper segments of a hair follicle, which was reported to be approximately 30 kPa (±23 kPa).[18] The estimated elastic modulus of PEGDA 3500 15% (S3) was found to be higher than the elastic modulus of the native hair follicle, so the 15% (S3) array was not ideal for the DP cells. In contrast, the estimated elastic moduli of PEGDA 3500 5% (S1) and 10% (S2) were much closer and within the range of the elastic modulus of the native hair follicle, so the DP cells might have adapted to the soft substrates and modulated their differentiations.

Conclusions

This work highlighted the effect of mechano-physical properties of the substrate on the behavior and differentiation of DP aggregates in 3D microgels. Expressions of important DP inductivity markers relating to WNT, BMP and FGF signaling

were shown to be more favorably expressed in DP aggregates cultured on softer substrates. The intricacy of spatial cues the matrix provides may have a deep impact on cell development. By understanding this property, 3D cultures can serve a greater purpose in enhancing the cellular response elicited from the DP cells for future *in vitro* hair follicle engineering pursuits.

Conflicts of interest

There are no conflicts to declare.

Acknowledgements

This study was supported by research grants from the Singapore National Additive Manufacturing Innovation Cluster (NAMIC) grant 2016011 and Singapore Academic Research Fund (AcRF) Tier 1 grant R148-000-224-112. The authors would like to thank Professor Mike Philpott and Dr Adiam Bahta from Queen Mary University London for kindly providing us with the immortalised human dermal papilla cells. The authors would also like to thank the following persons for their kind assistance in the work: Ms David Packiaraj Sheela from Life Sciences Institute at the National University of Singapore (NUS), and Ms Sue Li Chan and Ms Janice Tan from Anton Paar Singapore Pte Ltd.

References

1 K. D. Kaufman, *Mol. Cell. Endocrinol.*, 2002, **198**, 89–95.
2 F. Jiménez-Acosta and I. Ponce, *Actas Dermosifiliogr*, 2010, **101**, 291–306.
3 R. M. Bernstein and W. R. Rassman, *Dermatol. Clin.*, 2005, **23**, 393–414.
4 C. A. Jahoda, K. A. Horne and R. F. Oliver, *Nature*, 1984, **311**, 560–562.
5 A. Osada, T. Iwabuchi, J. Kishimoto, T. S. Hamazaki and H. Okochi, *Tissue Eng.*, 2007, **13**, 975–982.
6 F. H. Epstein, R. Paus and G. Cotsarelis, *N. Engl. J. Med.*, 1999, **341**, 491–497.
7 J. Kishimoto, R. Ehama, L. Wu, S. Jiang, N. Jiang and R. E. Burgeson, *Proc. Natl. Acad. Sci. U. S. A.*, 1999, **96**, 7336–7341.
8 T.-H. Young, C.-Y. Lee, H.-C. Chiu, C.-J. Hsu and S.-J. Lin, *Biomaterials*, 2008, **29**, 3521–3530.
9 C. A. Higgins, G. D. Richardson, D. Ferdinando, G. E. Westgate and C. A. B. Jahoda, *Exp. Dermatol.*, 2010, **19**, 546–548.
10 Y.-C. Huang, C.-C. Chan, W.-T. Lin, H.-Y. Chiu, R.-Y. Tsai, T.-H. Tsai, J.-Y. Chan and S.-J. Lin, *Biomaterials*, 2013, **34**, 442–451.
11 J. Kishimoto, R. E. Burgeson and B. A. Morgan, *Genes Dev.*, 2000, **14**, 1181–1185.
12 C.-M. Yen, C.-C. Chan and S.-J. Lin, *Biomaterials*, 2010, **31**, 4341–4352.
13 C.-H. Hsieh, J.-L. Wang and Y.-Y. Huang, *Acta Biomater.*, 2011, **7**, 315–324.
14 J. Pan, S. Yung Chan, J. E. A. Common, S. Amini, A. Miserez, E. Birgitte Lane and L. Kang, *J. Biomed. Mater. Res., Part A*, 2013, **101**, 3159–3169.
15 S. R. Caliari and J. A. Burdick, *Nat. Methods*, 2016, **13**, 405–414.
16 E. M. Ahmed, *J. Adv. Res.*, 2015, **6**, 105–121.
17 C.-C. Yang and G. Cotsarelis, *J. Dermatol. Sci.*, 2010, **57**, 2–11.
18 T. Bornschlögl, L. Bildstein, S. Thibaut, R. Santoprete, F. Fiat, G. S. Luengo, J. Doucet, B. A. Bernard and N. Baghdadli, *Proc. Natl. Acad. Sci. U. S. A.*, 2016, **113**, 5940–5945.
19 K. P. Menard, *Dynamic Mechanical Analysis: A Practical Introduction*, Boca Raton, Florida, 2nd edn, 2008.
20 M. A. Meyers and K. K. Chawla, *Mechanical behavior of materials*, Cambridge University Press, Cambridge, New York, 2nd edn, 2009.
21 M. Helvatjoglu-Antoniades, Y. Papadogiannis, R. S. Lakes, P. Dionysopoulos and D. Papadogiannis, *Dent. Mater.*, 2006, **22**, 450–459.
22 E. G. Y. Chew, J. H. J. Tan, A. W. Bahta, B. S.-Y. Ho, X. Liu, T. C. Lim, Y. Y. Sia, P. L. Bigliardi, S. Heilmann, A. C. A. Wan, M. M. Nöthen, M. P. Philpott and A. M. Hillmer, *J. Invest. Dermatol.*, 2016, **136**, 1559–1567.
23 L. Kang, M. J. Hancock, M. D. Brigham and A. Khademhosseini, *J. Biomed. Mater. Res., Part A*, 2010, **93**, 547–557.
24 S. L. Kieweg, A. R. Geonnotti and D. F. Katz, *J. Pharm. Sci.*, 2004, **93**, 2941–2952.
25 M. Ohyama and O. Veraitch, *J. Dermatol. Sci.*, 2013, **70**, 78–87.
26 O. Veraitch, T. Kobayashi, Y. Imaizumi, W. Akamatsu, T. Sasaki, S. Yamanaka, M. Amagai, H. Okano and M. Ohyama, *J. Invest. Dermatol.*, 2013, **133**, 1479–1488.
27 T. Kobayashi, A. Fujisawa, M. Amagai, T. Iwasaki and M. Ohyama, *Vet. Dermat.*, 2011, **22**, 414–422.
28 D. Enshell-Seijffers, C. Lindon, M. Kashiwagi and B. A. Morgan, *Dev. Cell*, 2010, **18**, 633–642.
29 V. A. Botchkarev and J. Kishimoto, *J. Invest. Dermatol. Symp. Proc.*, 2003, **8**, 46–55.
30 S. E. Millar, *J. Invest. Dermatol.*, 2002, **118**, 216–225.
31 R. Sennett and M. Rendl, *Semin. Cell Dev. Biol.*, 2012, **23**, 917–927.
32 V. A. Botchkarev and A. A. Sharov, *Differentiation*, 2004, **72**, 512–526.
33 L. Guo, L. Degenstein and E. Fuchs, *Genes Dev.*, 1996, **10**, 165–175.
34 H. Ohuchi, H. Tao, K. Ohata, N. Itoh, S. Kato, S. Noji and K. Ono, *Biochem. Biophys. Res. Commun.*, 2003, **302**, 562–567.
35 J. Y. Wong, A. Velasco, P. Rajagopalan and Q. Pham, *Langmuir*, 2003, **19**, 1908–1913.
36 T. Yeung, P. C. Georges, L. A. Flanagan, B. Marg, M. Ortiz, M. Funaki, N. Zahir, W. Ming, V. Weaver and P. A. Janmey, *Cell Motil. Cytoskeleton*, 2005, **60**, 24–34.

37 A. J. Engler, S. Sen, H. L. Sweeney and D. E. Discher, *Cell*, 2006, **126**, 677–689.
38 D. A. Rennerfeldt, A. N. Renth, Z. Talata, S. H. Gehrke and M. S. Detamore, *Biomaterials*, 2013, **34**, 8241–8257.
39 R.-Z. Lin, L.-F. Chou, C.-C. M. Chien and H.-Y. Chang, *Cell Tissue Res.*, 2006, **324**, 411–422.
40 J. S. Park, J. S. Chu, A. D. Tsou, R. Diop, Z. Tang, A. Wang and S. Li, *Biomaterials*, 2011, **32**, 3921–3930.